

<https://doi.org/10.3799/dqkx.2021.238>



新生逆冲断裂地表垂直位错分布与断层活动性关系:以河西走廊临泽断裂为例

李占飞^{1,2,3},徐锡伟^{1*},任俊杰¹,李康¹,康文君¹

1. 应急管理部国家自然灾害防治研究院,北京 100085

2. 北京市地震局,北京 100080

3. 中国地震局地质研究所,北京 100029

摘要: 活动断裂地表位错定量研究对理解断裂活动习性和构建多周期地震复发模型有重要意义。前人基于高精度地形数据对断裂地表位错分布开展了大量定量研究,但是关于累积位错变形沿新生逆冲断层的走向分布特征依然不清楚。本文选择河西走廊内部新生临泽逆冲断裂(<20 ka)为例,利用UAV (unmanned aerial vehicle)航测方法采集了断裂沿线约8 km长、2.5 km宽的高精度(0.5 m)地形数据,开展了精细地貌填图(1:500)、断层垂直位错测量(73个)、断层活动定量参数分析以及野外地质调查等工作。研究揭示,新生临泽逆冲断裂主要由2条左阶展布分支逆冲断层组成(L1和L2),阶区宽度约260 m。位错测量揭示,断层最大和最小累积位错分别为4.5 m和0.2 m,累积垂直位错呈明显不对称三角形分布,断层上位移亏损点与断层几何形态变化区域明显对应。断裂位错定量参数分析显示,临泽断裂结构不成熟,两个分支断裂后期会在破裂长度和位错增加下逐渐贯通。因此,可能需要注意后期强震活动造成新生逆冲断层向盆地内部拓展,及其对邻近城镇带来的直接和衍生灾害效应。

关键词: 新生逆冲断裂;垂直位错分布;结构成熟度;断层拓展;地震学。

中图分类号: P65

文章编号: 1000-2383(2022)03-831-13

收稿日期: 2021-08-16

Vertical Slip Distribution along Immature Active Thrust and Its Implications for Fault Evolution: A Case Study from Linze Thrust, Hexi Corridor

Li Zhanfei^{1,2,3}, Xu Xiwei^{1*}, Ren Junjie¹, Li Kang¹, Kang Wenjun¹

1. National Institute of Natural Hazard, Ministry of Emergency Management of the People's Republic of China, Beijing 100085, China

2. Beijing Earthquake Agency, Beijing 100080, China

3. Institute of Geology, China Earthquake Administration, Beijing 100029, China

Abstract: Slip distribution is necessary for the understanding and construction of rupture behavior along active faults. Although large number of researches have been focused on this issue using high-resolution topographic data, the slip distribution along

基金项目: 国家自然科学基金项目(Nos. 41941016, U1839204);国家自然科学重点基金项目(No. KFZD-SW-422);应急管理部国家自然灾害防治研究院基础科研经费项目(No. ZDJ2019-19)。

作者简介: 李占飞(1989—),男,博士研究生,主要从事活断层探测研究。ORCID: 0000-0003-4044-1348. E-mail: 876657683@qq.com

*通讯作者:徐锡伟,ORCID: 0000-0002-8301-7347. E-mail: xiweixu@vip.sina.com

引用格式: 李占飞,徐锡伟,任俊杰,李康,康文君,2022.新生逆冲断裂地表垂直位错分布与断层活动性关系:以河西走廊临泽断裂为例.地球科学,47(3):831—843.

Citation: Li Zhanfei, Xu Xiwei, Ren Junjie, Li Kang, Kang Wenjun, 2022. Vertical Slip Distribution along Immature Active Thrust and Its Implications for Fault Evolution: A Case Study from Linze Thrust, Hexi Corridor. *Earth Science*, 47(3):831—843.

immature active thrusts is still unclear. Two significantly different scenarios exist on this issue until this day. One is the large variation triangular distribution, and the other is comparatively uniform distribution. Using 8 km length, 2.5 km width and 0.5 m resolution UAV derived DEM data; we mapped in detail the geomorphic units, measured 73 vertical separations, and analyzed the parameters of the surface rupture. The Linze thrust is mainly composed of two left stepping branches, and the width of the step is ~ 260 m. The triangular slip distribution, with maximum and minimum vertical throws of 4.5 m and 0.2 m, respectively, reveals progressively lateral propagation of the thrust. The analysis of surface rupture parameters for the Linze thrust reveals the immature structure and the trend of connection and propagation of the segmented branches. Thus, more attention possibly should be paid to the influence of the propagation and connection of the thrust for the neighboring counties.

Key words: immature active thrust; vertical slip distribution; structure maturity; fault propagation; seismology.

0 引言

随着高精度地形测绘技术不断发展,前人对地表微构造地貌变形刻画越来越精细(Zielke *et al.*, 2010; Klinger *et al.*, 2011; 刘静等, 2013; Ren *et al.*, 2016; Chen *et al.*, 2018; Kang *et al.*, 2020).利用高精度地形数据前人在世界主要走滑断裂开展了大量活动断裂定量研究,清晰刻画了历次地震活动造成的地表变形沿断层走向变化,这些研究也为揭示断裂活动习性提供了大量基础数据(Klinger *et al.*, 2011; Ren *et al.*, 2016; Kang *et al.*, 2020).但是,关于断层位移沿走向的变化依然存在争议(Zielke *et al.*, 2010; Klinger *et al.*, 2011; Ren *et al.*, 2016; Manighetti *et al.*, 2020).对走滑断裂的定量研究显示,断层位移尤其是同震位移沿断层可能是均衡稳定的,只是存在局部微小变化(Klinger *et al.*, 2011; Ren *et al.*, 2016; Chen *et al.*, 2018; Kang *et al.*, 2020).但是也有结果揭示断层位移沿走向可能存在明显波峰,呈不对称三角形展布(Guo *et al.*, 2019; Manighetti *et al.*, 2020).其中,对正断层的断层位移分布研究更揭示出断层位移沿走向存在明显变化(Manighetti *et al.*, 2005; Manighetti *et al.*, 2015).前人通过系统总结世界主要活动断层的位移分布和破裂参数等定量参数认为,断层的破裂长度以及位移规模等可能与断层的几何结构和成熟度等密切相关(Manighetti *et al.*, 2007; Wesnousky, 2008; Manighetti *et al.*, 2015).

前人在走滑断层、正断层上开展了大量地表破裂滑动位移分布定量研究,但是针对逆断层研究相对较少,尤其是新生逆断层。这一方面源于逆断层变形相对复杂,既有垂直位错变形又有褶皱挠曲等变形,断层陡坎类型较多(Philip *et al.*, 1992; Xu *et al.*, 2009; Yu *et al.*, 2010),这为逆断层变形的精细定量研究带来了困难。其次,逆断层变形在地表

不仅存在向两侧拓展,更存在向前陆盆地内部的拓展(Tappognier *et al.*, 1990; Zuza *et al.*, 2016; Hu *et al.*, 2019)。这种拓展过程使逆断层地表变形更加弥散,识别和区分断层历次地震活动造成的垂直位移更加困难(Xu *et al.*, 2009)。因此,前人只在屈指可数的逆断层上开展过系统的地表位错定量研究,如合黎山南麓断裂(Bi *et al.*, 2018)、新疆独山子断裂(Wei *et al.*, 2020)、以及佛洞庙-红崖子断裂(Huang *et al.*, 2021)等。这些研究为逆断层的大地震复发模型、同震地表破裂特征以及断裂带发育与演化等提供了重要参考。

但是,前人研究主要集中在活动时间相对较早的(>5 Ma)的活动逆冲断裂上,断裂成熟度相对较高,断裂不同分支之间通过多次地震活动基本连通(Manighetti *et al.*, 2007, 2015)。因此,断裂垂直位错沿走向变化相对较小,呈现基本均一的状态(Bi *et al.*, 2018; Wei *et al.*, 2020; Huang *et al.*, 2021)。那么,新生逆冲断裂累积垂直位错分布特征如何?它的几何形态如何?垂直位错分布与断裂几何形态及断层发育演化有何关系?为了研究上述问题,本文以祁连山北麓逆冲断裂向盆地内部拓展新生的扭性临泽断裂(<20 ka)为例,利用UAV技术采集了断裂沿线高精度地形数据(0.5 m)。基于高精度地形数据,开展了断裂沿线精细地貌填图(1:500),利用3D_faults_offset方法开展了断裂沿线密集累积垂直位错测量(Stewart *et al.*, 2018),并对获得的断层几何结构和垂直位错进行了野外验证。结果显示,新生临泽逆冲断裂由2条呈左阶展布的分支断层组成,在断层上盘发育小型正断层。断层垂直位错表现出明显不对称三角形分布,断层中局部位错亏损点与断层几何形态变化区对应。对断层位错与破裂长度等定量参数的分析表明,临泽断裂将会向两侧拓展,分支之间随着破裂长度和位错增加逐渐贯通,位于

河西走廊盆地内部的城镇可能需要注意拓展新生逆冲断层带来的地震及其衍生灾害影响。

1 构造背景

新生代以来由于印度板块和欧亚板块之间的挤压碰撞,构造变形向高原内部渐进式拓展,造成了青藏高原东北缘的祁连山及河西走廊地区发育了大量典型板块内部逆冲断裂系,如玉门断裂、佛洞庙-红崖子断裂、榆木山北麓断裂、民乐-大马营断裂以及武威盆地南缘断裂等(Tapponnier *et al.*, 1990; 中国地震局地质研究所和中国地震局兰州地震研究所, 1993; Gaudemer *et al.*, 1995; Zhang *et al.*, 2004; 杨树锋等, 2007; Xu *et al.*, 2010; Zheng *et al.*, 2013; Xiong *et al.*, 2017; Yang *et al.*, 2018; Liu *et al.*, 2019; Hetzel *et al.*, 2019; 陈宣华等, 2019)(图1)。正是由于这种显著地壳缩短变形($\sim 5\text{--}7 \text{ mm/a}$)(Zhang *et al.*, 2004; Liang *et al.*, 2013; Zheng *et al.*, 2013)和逆断层发育,造成了河西走廊地区5次显著地表破裂型地震(Xu *et al.*, 2010; Allen *et al.*, 2017)。因此,河西走廊地区具有相对较高地震危险性,断裂活动行为定量研究对该区地震危险性评估有重要意义。

临泽断裂位于榆木山北麓民乐盆地内部(图1),与榆木山主断裂相似,断裂活动以逆冲变形为

主,局部具有右旋走滑分量(Ren *et al.*, 2019; 庞炜等, 2019),为一条压扭性质活动断裂。前人在断裂上开展过相关定量研究(Palumbo *et al.*, 2009; 金卿等, 2011; 庞炜等, 2019)。通过对断裂进行古地震研究,揭示出断裂 $\sim 10 \text{ ka}$ 以来发生过4次古地震事件,全新世以来发生过3次古地震事件,临泽断裂全新世以来活动比较强烈(庞炜等, 2019)。通过差分GPS测量前人揭示断裂上存在明显断层陡坎,陡坎高度 $0.2\text{--}4.1 \text{ m}$ (Palumbo *et al.*, 2009; 庞炜等, 2019)。前人的初步定量研究揭示出,临泽断裂为一条盆地内部新生逆冲断裂($<20 \text{ ka}$),断层几何结构和构造变形相对简单,表现为显著的逆冲垂直位错变形(Palumbo *et al.*, 2009; 金卿等, 2011; 庞炜等, 2019)。这为开展新生逆冲断裂的精细几何结构特征、密集累积垂直位错测量及断层发育演化过程研究提供了天然条件。

2 数据和方法

祁连山北麓河西走廊地区地处干旱半干旱地区,降雨量相对较少,地表植被覆盖率较低(Ta *et al.*, 2004)。因此,采用UAV航测方法,通过原始影像数据采集、控制点测量以及空三矫正是步骤,获得了临泽断裂约8 km长,2.5 km宽,0.5 m精度的DEM(digital elevation model)数据(图2)。利用

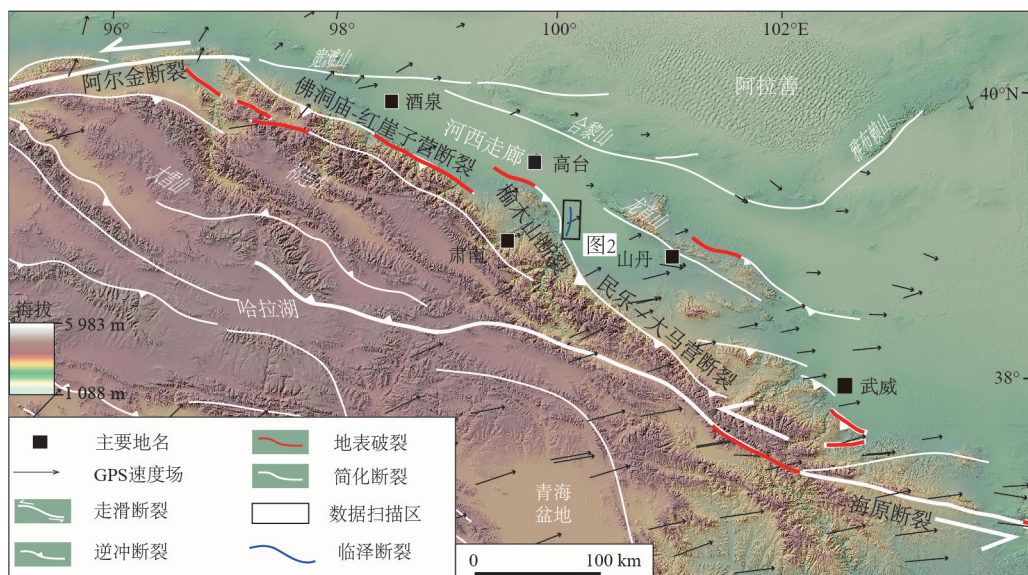


图1 临泽断裂及其周缘活动构造图

Fig.1 Active tectonic map around Linze thrust

白色线段为断层,断层数据源自Xu *et al.* (2010)。黑色箭头代表GPS速度场,数据源自Liang *et al.* (2013)。红色线段为地表破裂带,数据源自Xu *et al.* (2010)。蓝色线段为本文研究对象临泽断裂,黑框为UAV数据扫描区

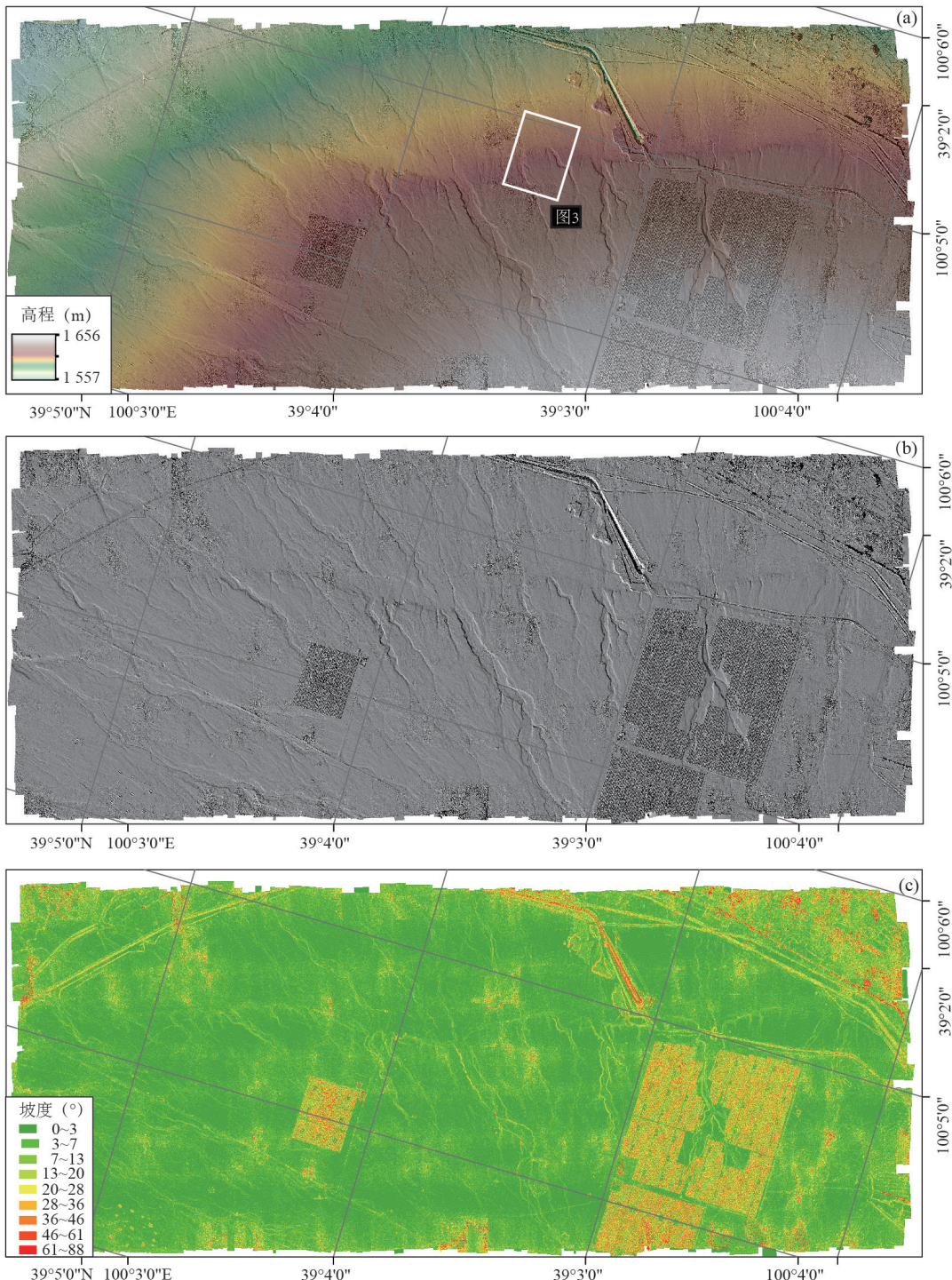


图2 临泽断裂区域获得的高精度(0.5 m)地形数据

Fig.2 High-resolution topographic (0.5 m) data along Linze thrust
白色方框为图3位置; a. DEM图; b. 山影图; c. 坡度图

GIS 平台对数据进行了山影、坡度及不同角度地形剖面线提取。综合不同洪积扇切割关系、地貌因子特征以及已有测年结果(庞炜等, 2019), 对研究区进行了 1:500 的精细地貌填图。同时, 通过野外地质调查对填图结果进行了验证(图 3d)。

断层垂直位错测量主要采用 3D_fault_offsets 方法进行(Stewart *et al.*, 2018)。该方法能够基于人工选择的断层上下盘矩形区域和断层位置, 利用 9 个不同地貌线指标, 采用蒙特卡托模拟方法, 快速自动化获得断层垂直位错值(图 3)。同时, 该方法能够

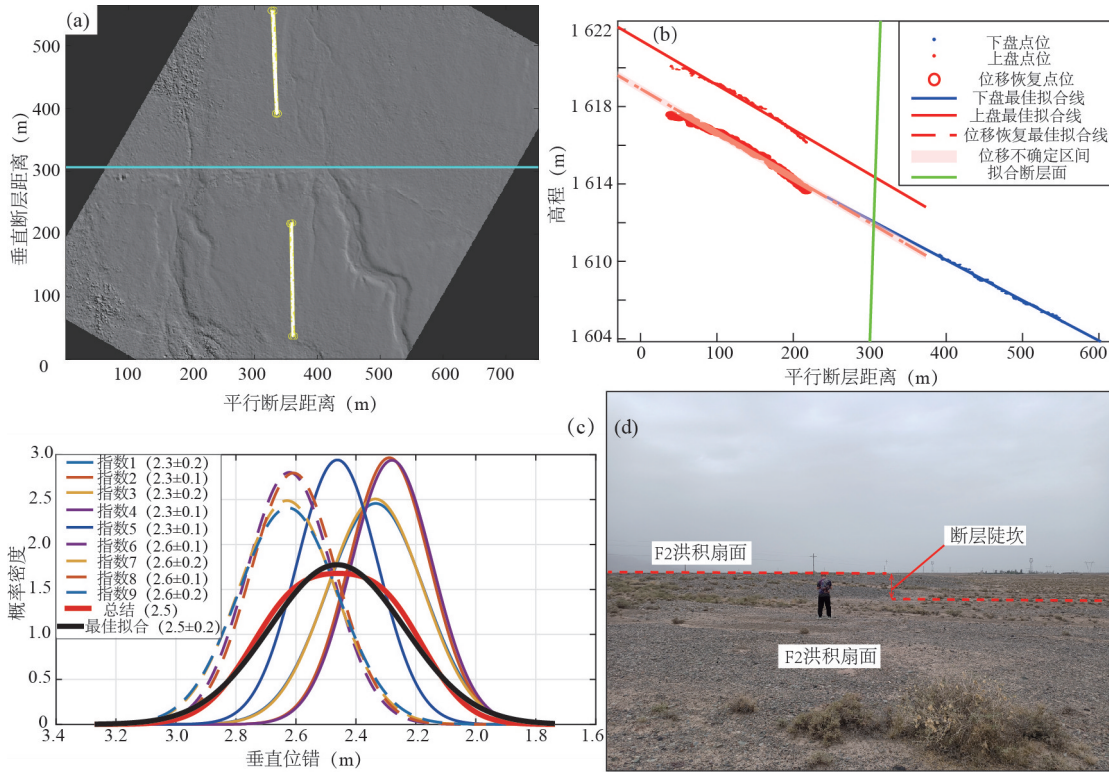


图3 典型地貌点(P-34)的3D fault offset测量示例与野外验证

Fig.3 An example (P-34) of throw measurement and its filed verification

a. 垂直位错测量中断层走向与测量矩形选择; b. 垂直位错自动恢复; c. 基于9种地貌参数的垂直位错拟合; d. 垂直位错测量的野外验证

充分考虑断层倾角、走向、数据分辨率等对断层位错测量结果的影响,给出最佳位错值和误差(图3),被广泛地应用于断裂地表位错测量中(Stewart *et al.*, 2018; Yao *et al.*, 2019; 康文君等, 2020)。垂直位错测量时,逆断层倾角依据前人研究结果设置为 $50^{\circ}\pm 10^{\circ}$,断层上盘正断层倾角设置为 $60^{\circ}\pm 10^{\circ}$ (庞炜等, 2019)(表1)。断层上下盘测量矩形区的选择充分考虑精细填图结果,避开侵蚀和后期加积区域,选择断层上下盘同期地貌面开展(图3)。同时,使测量线位于主断裂位置,相对远离断层陡坎,且剖面线足够长,使获得的垂直位错更加可靠(Liu *et al.*, 2019)(图3)。

3 结果与讨论

3.1 断裂精细断错地貌特征与垂直位错分布

通过填图揭示出断裂沿线共存在3期地貌面分别为F1、F2、F3。其中F1为最新一期常年流水冲洪积扇,F2为侵蚀冲沟深度约0.5 m的洪积扇,与F1为侵蚀切割关系。F3为区域内分布最广泛的最老一期冲洪积扇,侵蚀冲沟的深度约0.7 m,与F2呈相互切割关系(图4)。断裂整体线

性明显,走向N 165° E,倾角 $50^{\circ}\pm 10^{\circ}$ (庞炜等, 2019),由2条呈左阶展布的分支断层组成,阶步宽度约260 m。两条分支断层内部又由长度约1.2 km小分支断层组成且呈左阶展布。在断层上盘,发育典型的由于断层倾角变化形成局部拉张环境所形成的正断层(Tapponnier *et al.*, 1990; Avouac *et al.*, 1993)(图4)。由GPS速度场揭示(Liang *et al.*, 2013),断裂走向与远场应力场明显斜交,断裂左阶的几何结构可能反映了这种斜交状态产生的右旋运动趋势(庞炜等, 2019)(图5a)。

73个累积垂直位错测量结果揭示,垂直位错总体呈不对称三角形分布,最大垂直位错为4.5 m,最小位错值为0.2 m(图5和表1)。所有垂直位错测量点都位于F3地貌面主断裂位置,在断裂上盘测量获得了1.0~4.5 m的正断位错分量(图5)。具体来看,断层的垂直位错分布与两条分支逆冲断裂(L1和L2)相对应,存在两个明显波峰。在0~3.6 km范围L1分支断裂发育区,最大位错出现在3.1 km处,位错值为4.5 m。沿L1分支断层两侧,断层垂直位错分别在0 km和3.6 km处线性衰减为0.6 m和0.7 m

(图 5). 在 3.6~7.5 km 范围 L2 分支断裂展布区, 最大垂直位错 4.4 m 位于 5.3 km 处, 累积垂直位错向断层两侧在 3.6 km 和 7.5 km 处分别衰减为 0.7 m 和 0.3 m. 因此, 位错分布在 L1、L2 分支断层内部, 同样表现出不对称三角形分布.

断裂几何形态与垂直位错对比分析表明, 断裂分支阶步位置(3.5~4.2 km)与垂直位错亏损区域对应(图 5). 断裂几何形态复杂区与位移亏损的对应性在其他活动断裂广泛发育(Zhang *et al.*, 1999; Duan and Oglesby, 2006; Manighetti *et al.*, 2007, 2015; Wesnousky, 2008). 数值模拟分析表明这些

位移亏损区恰好位于静态应力集中分布区, 对断层活动起着重要控制作用(Duan and Oglesby, 2006; Manighetti *et al.*, 2007, 2015). 对比位错分布与断裂沿线走向分布结果表明, 垂直位错变化与断裂走向角度变化具有协调性(图 5c). 例如, 在沿断层距离的 5~6 km 处, 断层垂直位错的衰减与断层走向变化有较好对应性. 同时, 该位置与 L2 分支断层内部呈弧形左阶展布小分支断层的阶区位置相对应(图 5). 因此, 这些对比表明, 断裂几何形态对断层的地表构造变形起着重要控制作用. 断层几何形态变化区, 往往对应于位移亏损区.

表 1 临泽断裂垂直位错测量结果

Table 1 Vertical offset measurements results along Linze thrust

编号	纬度 N	经度 E	距离 (m)	断层走向 NE(°)	倾角 (°)	倾角误差 (°)	位错值 (m)	误差 (m)	地貌面
0	39° 5' 30.733"	100° 4' 10.503"	0	169	50	10	0.6	0.1	F2
1	39° 5' 26.137"	100° 4' 12.071"	142	174	50	10	1	0.1	F2
2	39° 5' 21.200"	100° 4' 11.674"	309	190	50	10	1.7	0.2	F2
3	39° 5' 15.774"	100° 4' 10.302"	476	189	50	10	0.2	0.2	F2
4	39° 5' 11.685"	100° 4' 10.193"	607	159	50	10	0.9	0.2	F2
5	39° 5' 6.949"	100° 4' 11.854"	743	141	50	10	2.3	0.1	F2
6	39° 5' 4.707"	100° 4' 15.390"	846	153	50	10	2.7	0.1	F2
7	39° 5' 1.149"	100° 4' 16.562"	975	158	50	10	2.4	0.1	F2
8	39° 4' 58.190"	100° 4' 17.899"	1 050	157	50	10	3.8	0.2	F2
9	39° 4' 54.723"	100° 4' 19.618"	1 167	160	50	10	1.7	0.1	F2
10	39° 4' 51.609"	100° 4' 21.583"	1 279	159	50	10	1.2	0.2	F2
11	39° 4' 48.927"	100° 4' 22.820"	1 374	158	50	10	1.2	0.2	F2
12	39° 4' 46.364"	100° 4' 23.339"	1 460	150	50	10	2.1	0.2	F2
13	39° 4' 42.359"	100° 4' 26.337"	1 607	150	50	10	2.8	0.1	F2
14	39° 4' 39.744"	100° 4' 28.014"	1 707	145	50	10	3	0.1	F2
15	39° 4' 37.681"	100° 4' 28.862"	1 773	166	50	10	2.3	0.1	F2
16	39° 4' 34.802"	100° 4' 29.411"	1 865	165	50	10	2.3	0.2	F2
17	39° 4' 32.413"	100° 4' 30.280"	1 950	156	50	10	3.8	0.1	F2
18	39° 4' 30.269"	100° 4' 31.172"	2 028	164	50	10	2.7	0.1	F2
19	39° 4' 27.502"	100° 4' 31.344"	2 112	161	50	10	2.1	0.2	F2
20	39° 4' 24.157"	100° 4' 32.466"	2 239	161	50	10	1.7	0.1	F2
21	39° 4' 20.572"	100° 4' 32.348"	2 356	185	50	10	2.9	0.2	F2
22	39° 4' 16.836"	100° 4' 31.192"	2 491	191	50	10	2.9	0.1	F2
23	39° 4' 13.686"	100° 4' 30.199"	2 584	175	50	10	4	0.2	F2
24	39° 4' 10.610"	100° 4' 32.145"	2 679	178	50	10	3.2	0.2	F2
25	39° 4' 0.537"	100° 4' 31.277"	2 998	175	50	10	3	0.2	F2
26	39° 3' 57.045"	100° 4' 33.341"	3 106	178	50	10	4.4	0.4	F2
27	39° 3' 53.598"	100° 4' 33.113"	3 219	170	50	10	4.5	0.3	F2
28	39° 3' 49.077"	100° 4' 33.475"	3 359	165	50	10	2.1	0.1	F2
29	39° 3' 41.619"	100° 4' 35.108"	3 595	161	50	10	0.7	0.1	F2
30	39° 3' 38.216"	100° 4' 36.808"	3 704	152	50	10	1	0.1	F2
31	39° 3' 35.084"	100° 4' 37.448"	3 825	154	50	10	1.6	0.2	F2

续表1

编号	纬度 N	经度 E	距离 (m)	断层走向 NE(°)	倾角 (°)	倾角误差 (°)	位错值 (m)	误差 (m)	地貌面
32	39° 3' 34.382"	100° 4' 47.025"	3 912	151	50	10	0.8	0.1	F2
33	39° 3' 30.379"	100° 4' 50.060"	4 051	151	50	10	3.3	0.1	F2
34	39° 3' 28.199"	100° 4' 51.188"	4 127	149	50	10	2.5	0.2	F2
35	39° 3' 24.443"	100° 4' 53.794"	4 263	157	50	10	2.7	0.1	F2
36	39° 3' 21.040"	100° 4' 54.314"	4 367	172	50	10	2.8	0.1	F2
37	39° 3' 18.204"	100° 4' 54.598"	4 462	176	50	10	2.8	0.1	F2
38	39° 3' 10.995"	100° 4' 54.467"	4 695	166	50	10	3.9	0.2	F2
39	39° 3' 8.746"	100° 4' 55.506"	4 769	168	50	10	4	0.1	F2
40	39° 3' 5.682"	100° 4' 55.674"	4 869	168	50	10	3.5	0.2	F2
41	39° 3' 1.787"	100° 4' 56.538"	4 995	161	50	10	2.8	0.2	F2
42	39° 3' 0.022"	100° 5' 0.533"	5 077	164	50	10	2.6	0.2	F2
43	39° 2' 57.647"	100° 5' 2.312"	5 159	168	50	10	2.5	0.1	F2
44	39° 2' 54.040"	100° 5' 2.725"	5 274	168	50	10	3.5	0.2	F2
45	39° 2' 51.184"	100° 5' 3.121"	5 382	174	50	10	4.4	0.2	F2
46	39° 2' 43.744"	100° 5' 5.075"	5 619	148	50	10	2.2	0.2	F2
47	39° 2' 42.836"	100° 5' 7.833"	5 674	151	50	10	3	0.1	F2
48	39° 2' 39.958"	100° 5' 9.362"	5 776	133	50	10	4.3	0.1	F2
49	39° 2' 37.789"	100° 5' 9.871"	5 854	145	50	10	3.8	0.1	F2
50	39° 2' 35.932"	100° 5' 12.211"	5 934	147	50	10	3.1	0.1	F2
51	39° 2' 34.096"	100° 5' 13.585"	6 014	156	50	10	3.1	0.1	F2
52	39° 2' 31.842"	100° 5' 14.657"	6 102	162	50	10	2.8	0.1	F2
53	39° 2' 30.281"	100° 5' 15.090"	6 156	165	50	10	2.6	0.1	F2
54	39° 2' 27.567"	100° 5' 17.019"	6 235	167	50	10	2.6	0.1	F2
55	39° 2' 25.833"	100° 5' 20.420"	6 311	167	50	10	2.1	0.1	F2
56	39° 2' 24.125"	100° 5' 20.820"	6 371	173	50	10	0.7	0.1	F2
57	39° 2' 21.663"	100° 5' 20.890"	6 458	170	50	10	0.2	0.3	F2
58	39° 2' 19.349"	100° 5' 20.424"	6 528	167	50	10	1.5	0.1	F2
59	39° 2' 17.051"	100° 5' 17.861"	6 613	176	50	10	1.5	0.1	F2
60	39° 2' 12.581"	100° 5' 17.449"	6 755	174	50	10	0.1	0.2	F2
61	39° 2' 10.317"	100° 5' 20.121"	6 847	177	50	10	1.8	0.2	F2
62	39° 2' 7.953"	100° 5' 21.145"	6 931	184	50	10	2.4	0.3	F2
63	39° 2' 4.702"	100° 5' 20.878"	7 037	188	50	10	0.4	0.1	F2
64	39° 2' 1.498"	100° 5' 20.033"	7 142	185	50	10	0.3	0.3	F2
65	39° 5' 25.261"	100° 3' 42.254"	91	158	60	10	3.2	0.3	F2
66	39° 5' 21.777"	100° 3' 42.968"	205	157	60	10	4.3	0.3	F2
67	39° 5' 18.679"	100° 3' 43.910"	292	155	60	10	3.7	0.2	F2
69	39° 5' 12.253"	100° 3' 47.177"	508	148	60	10	4.5	0.1	F2
74	39° 4' 56.518"	100° 3' 57.976"	978	145	60	10	1	0.1	F2
76	39° 3' 52.685"	100° 4' 6.297"	2 998	139	60	10	1.8	0.1	F2
77	39° 3' 50.608"	100° 4' 8.444"	3 106	143	60	10	1.6	0.1	F2
78	39° 3' 48.414"	100° 4' 9.956"	3 219	135	60	10	1.3	0.1	F2

3.2 垂直位错分布揭示的断裂向盆地内部拓展生长

密集断层位错分布研究对理解断层拓展和滑动历史,以及发育与演化过程有重要意义(Cowie

and Scholz, 1992; Scholz *et al.*, 1993; Bürgmann *et al.*, 1994; Cheng *et al.*, 2020).前人基于地表位错测量和数值模拟分析,发现断裂生长拓展方向与累积垂直位错线性衰减方向相同,这种现象广泛存在

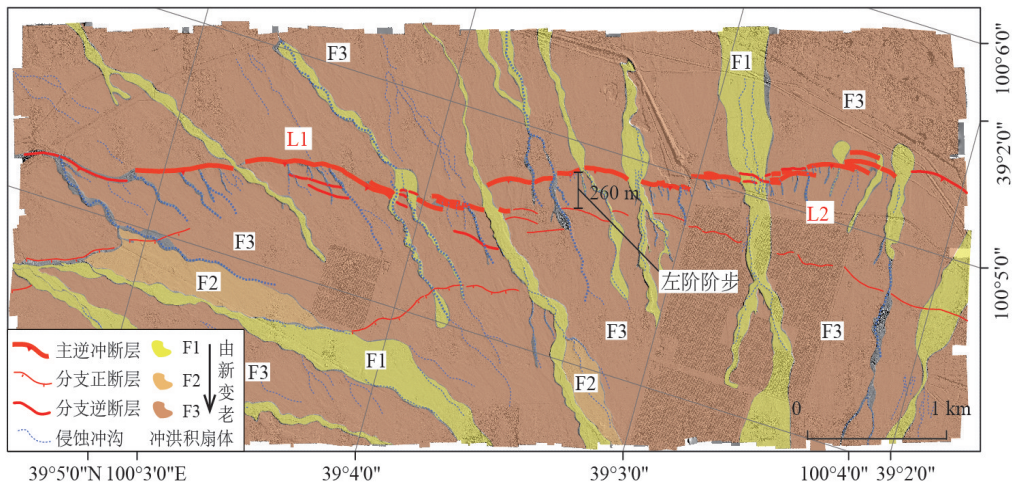


图 4 基于高精度地形数据的精细(1:500)断错地貌填图

Fig.4 Detailed geomorphic mapping based on high-resolution DEM data

红色线段为活动断裂，彩色矩形为不同期次地貌体

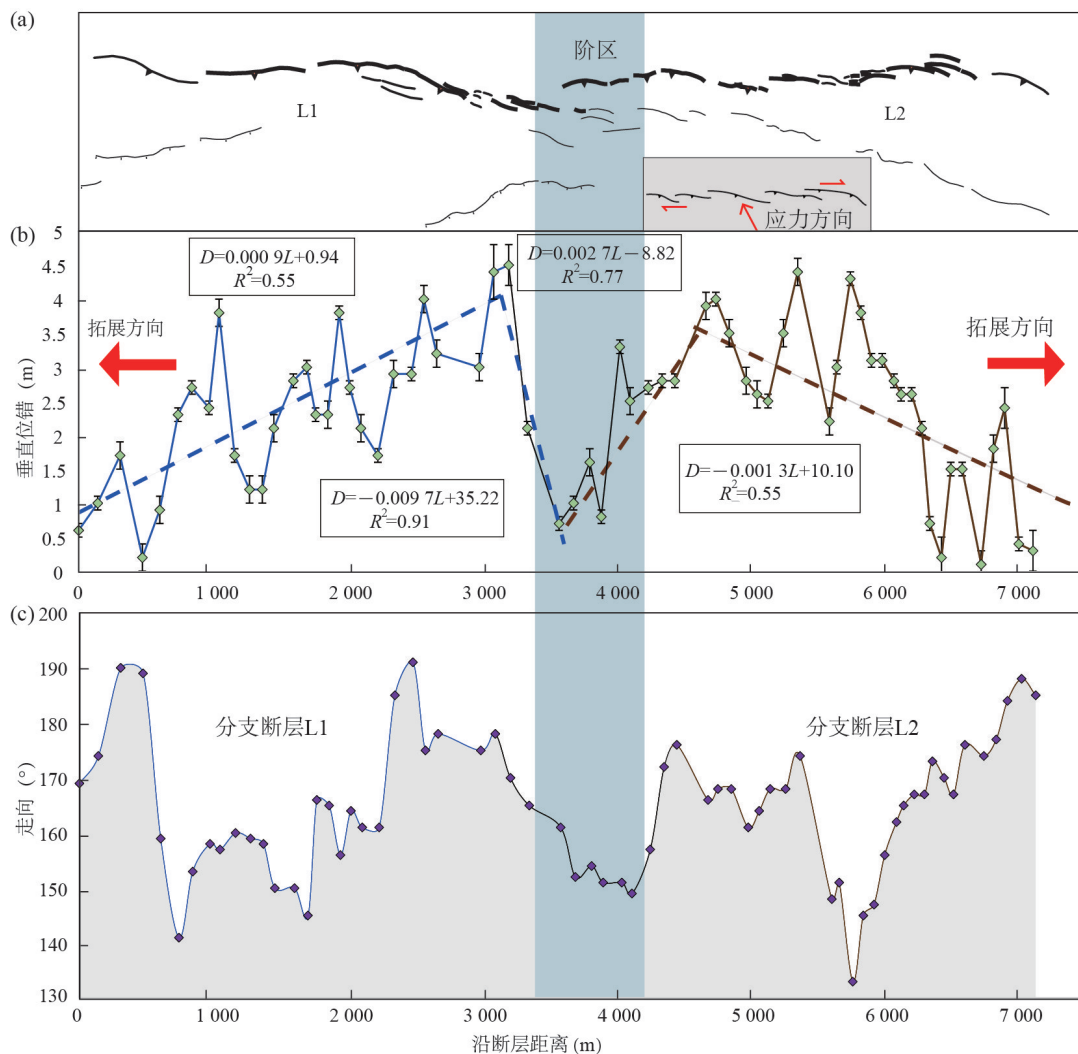


图 5 临泽断裂累积垂直位错分布及其与几何结构之间关系

Fig. 5 Throw distributions and its relationship with fault geometry

a. 断裂几何结构; b. 断裂垂直位错分布; c. 断裂走向分布

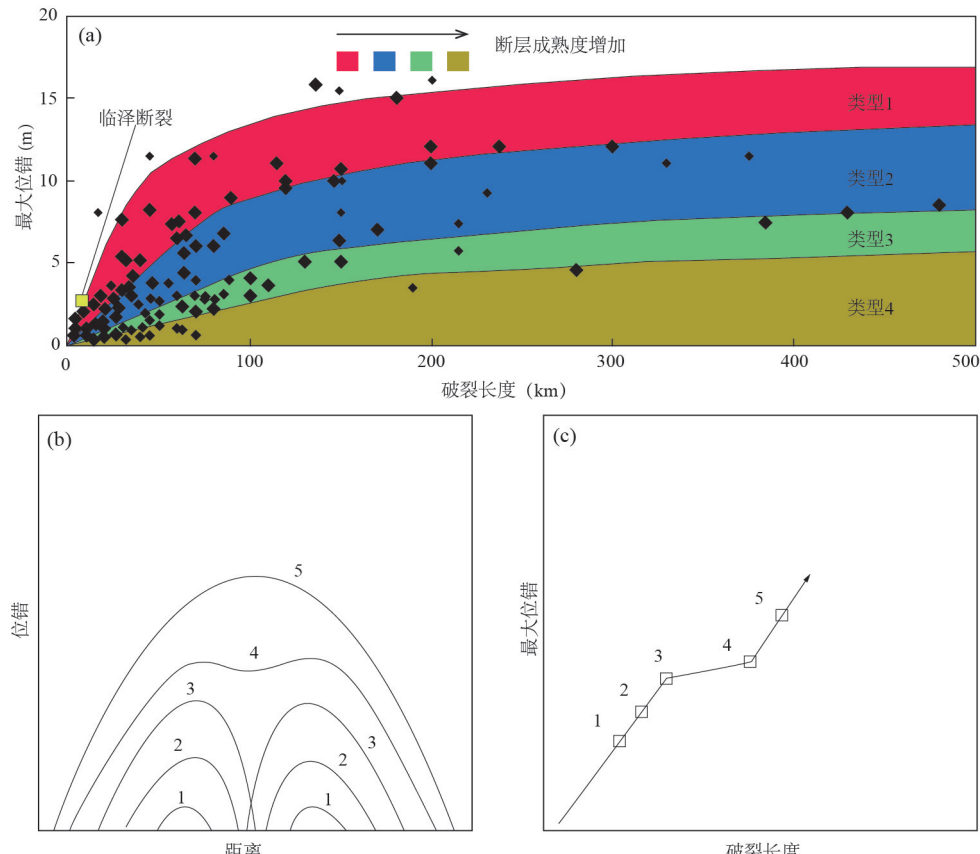


图6 临泽断裂定量参数分析与断层发育演化模式

Fig.6 The analysis of surface rupture parameters and evolution model for the Linze thrust

a. 断裂结构成熟度分析(修改自 Manighetti *et al.*, 2007); b. 分支断裂贯通发育模式; c. 破裂长度与最大位错演化模式, 修改自 Kim *et al.* (2000)

于主要活动断裂上(Cartwright *et al.*, 1995; Gupta and Scholz, 2000; Manighetti *et al.*, 2007, 2015). 临泽断裂位错测量数据分析表明, 断裂两侧位错沿断层走向存在明显线性衰减, 衰减系数在 L1 和 L2 分支断裂两侧分别为 9×10^{-4} 和 1.3×10^{-3} , 这充分揭示了临泽断裂随着时间演化将会继续向两侧拓展生长(图 5).

临泽断裂位错表现出明显不对称三角形分布, 这可能受控于断层结构成熟度相对较低, 并符合分支断裂相互贯通的生长机制. 虽然前人在研究活动断裂尤其是走滑断裂时指出, 断裂的位错分布表现出相对稳定的均一状态(Klinger *et al.*, 2011; Chen *et al.*, 2018; Kang *et al.*, 2020). 但也有部分研究尤其是针对正断层的研究揭示, 断层的地表垂直位错变形呈现明显的不对称三角形分布(Manighetti *et al.*, 2007, 2015). 关于断层三角形位错分布特征形成原因, 前人系统总结全球不同性质活动断裂位错分布特征, 认为这可能

与断裂几何结构的成熟度密切相关(Manighetti *et al.*, 2007, 2015), 并将断裂的成熟度依据最大位错值和破裂长度之间的相互关系分为 4 个等级(图 6)(Manighetti *et al.*, 2007). 当断裂相对年轻, 断层结构的成熟度相对较低时, 断裂不同段落之间相互分割, 断裂的最大位错与破裂长度之间的比值相对较大(Segall and Pollard, 1980; Cartwright *et al.*, 1995; Kim *et al.*, 2000).

依据本次定量研究获得的临泽断裂的破裂长度和最大垂直位错分别为 8 km 和 4.5 m, 依据断层倾角获得断裂的逆冲位移为 5.8 m. 将这些地表破裂参数与前人总结的成熟度对比可以看出, 临泽断裂属于“类型 1”即几何结构不成熟活动断裂. 因此, 临泽断裂三角形不对称型分布可能源于断裂活动时间相对较短、断裂的几何结构成熟度相对较低. 同时, 几何形态对垂直位错分布的显著控制作用及与分支断裂对应的双峰式位错分布表明(Kim *et al.*, 2000; Wilkins and Gross, 2002), 临泽断裂

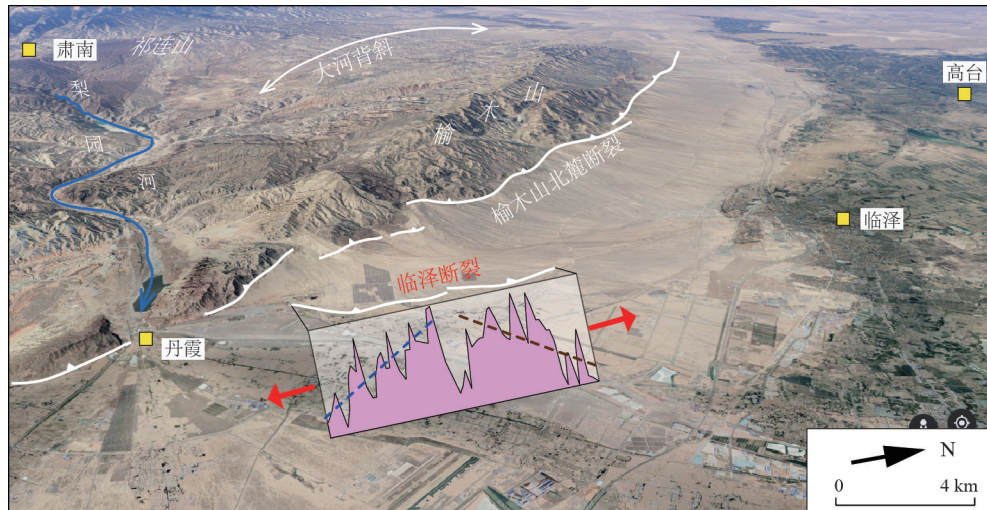


图 7 临泽断裂的拓展与周缘城镇分布

Fig.7 The propagation of Linze thrust and its surrounding counties

的发育与演化符合分支断层相互贯通机制，即断层的垂直位错分布与分支断裂对应，随着破裂长度增加和累积垂直位错增加，临泽断裂的两条分支断裂在向两侧拓展过程中相互贯通（Cowie and Scholz, 1992；Kim *et al.*, 2000）。

临泽断裂的这种可能向两侧位错线性衰减方向拓展的过程，在河西走廊地区的其他逆冲断裂上也有所揭示。例如，Bi *et al.* (2018) 在合黎山南缘断裂上的垂直位错测量研究认为，断裂的累积垂直位错存在着由西向东的递增趋势，由此初步推测断裂可能存在向西的拓展生长。同时，前人对祁连山北麓逆冲断裂系的精细地球物理探测和沉积盆地演化分析也揭示出，断裂存在向盆地内部的拓展，显著地吸收着青藏高原东北缘的地壳缩短变形（Ye *et al.*, 2015；Zuza *et al.*, 2016；Hu *et al.*, 2019）。

4 结论

本研究依据 UAV 扫描获得的约 8 km 的高精度地形数据定量研究揭示出，临泽断裂由 2 支呈左阶展布的逆冲分支断裂组成（L1 和 L2），分支断裂内部又由多条呈左阶展布的小分支断裂组成。断裂的这种几何结构可能代表了受局部应力场与断层倾角控制的压扭性构造变形。断裂垂直位错测量表明，累积垂直位错分布表现出明显不对称三角形分布，最大和最小垂直位错分别为 4.5 m 和 0.2 m。断层垂直位错的显著变化区域与几何结构变化区对应，揭示出断裂的几何结构对地表垂直构造变形起着重要控制作用。同时，临泽断裂位错

分布存在显著的向断层两侧线性衰减（衰减系数约 0.001），这种线性衰减代表了逆冲断裂向两侧的不断拓展。断裂的地表破裂参数分析表明，临泽断裂属于结构不成熟年轻活动断裂。断裂发育与演化可能遵循分支断裂相互贯通模型，随着断裂长度和累积垂直位错增加，分支断裂将会逐渐连通，断层几何结构变化带来的位移亏损逐渐消失。因此，可能需要注意断裂向盆地内部拓展对周边城镇带来的地震及其衍生灾害的影响（图 7）。

References

- Allen, M. B., Walters, R. J., Song, S., et al., 2017. Partitioning of Oblique Convergence Coupled to the Fault Locking Behavior of Fold-and-Thrust Belts: Evidence from the Qilian Shan, Northeastern Tibetan Plateau. *Tectonics*, 36(9–10): 1679–1698. <https://doi.org/10.1002/2017TC004476>
- Avouac, J. P., Tapponnier, P., Bai, M., et al., 1993. Active Thrusting and Folding along the Northern Tien Shan and Late Cenozoic Rotation of the Tarim Relative to Dzungaria and Kazakhstan. *Journal of Geophysical Research: Solid Earth*, 98(B4): 6755–6804. <https://doi.org/10.1029/92jb01963>
- Bi, H. Y., Zheng, W. J., Ge, W. P., et al., 2018. Constraining the Distribution of Vertical Slip on the South Heli Shan Fault (Northeastern Tibet) from High-Resolution Topographic Data. *Journal of Geophysical Research: Solid Earth*, 123(3): 2484–2501. <https://doi.org/10.1002/2017jb014901>
- Bürgmann, R., Pollard, D. D., Martel, S. J., 1994. Slip

- Distributions on Faults: Effects of Stress Gradients, Inelastic Deformation, Heterogeneous Host - Rock Stiffness, and Fault Interaction. *Journal of Structural Geology*, 16(12): 1675—1690. [https://doi.org/10.1016/0191-8141\(94\)90134-1](https://doi.org/10.1016/0191-8141(94)90134-1)
- Cartwright, J. A., Trudgill, B. D., Mansfield, C. S., 1995. Fault Growth by Segment Linkage: An Explanation for Scatter in Maximum Displacement and Trace Length Data from the Canyonlands Grabens of SE Utah. *Journal of Structural Geology*, 17(9): 1319—1326. [https://doi.org/10.1016/0191-8141\(95\)00033-A](https://doi.org/10.1016/0191-8141(95)00033-A)
- Chen, T., Jing, L. Z., Shao, Y. X., et al., 2018. Geomorphic Offsets along the Creeping Laohu Shan Section of the Haiyuan Fault, Northern Tibetan Plateau. *Geosphere*, 14(3): 1165—1186. <https://doi.org/10.1130/ges01561.1>
- Chen, X. H., Shao, Z. G., Xiong, X. S., et al., 2019. Early Cretaceous Overthrusting of Yumu Mountain and Hydrocarbon Prospect on the Northern Margin of the Qilian Orogenic Belt. *Acta Geoscientica Sinica*, 40(3): 377—392 (in Chinese with English abstract).
- Cheng, J., Rong, Y. F., Magistrale, H., et al., 2020. Earthquake Rupture Scaling Relations for Mainland China. *Seismological Research Letters*, 91(1): 248—261. <https://doi.org/10.1785/0220190129>
- Cowie, P. A., Scholz, C. H., 1992. Displacement-Length Scaling Relationship for Faults: Data Synthesis and Discussion. *Journal of Structural Geology*, 14(10): 1149—1156. [https://doi.org/10.1016/0191-8141\(92\)90066-6](https://doi.org/10.1016/0191-8141(92)90066-6)
- Duan, B. C., Oglesby, D. D., 2006. Heterogeneous Fault Stresses from Previous Earthquakes and the Effect on Dynamics of Parallel Strike-Slip Faults. *Journal of Geophysical Research: Solid Earth*, 111(B5): B05309. <https://doi.org/10.1029/2005jb004138>
- Gaudemer, Y., Tapponnier, P., Meyer, B., et al., 1995. Partitioning of Crustal Slip between Linked, Active Faults in the Eastern Qilian Shan, and Evidence for a Major Seismic Gap, the ‘Tianzhu Gap’, on the Western Haiyuan Fault, Gansu (China). *Geophysical Journal International*, 120(3): 599—645. <https://doi.org/10.1111/j.1365-246X.1995.tb01842.x>
- Guo, P., Han, Z. J., Dong, S. P., et al., 2019. Surface Rupture and Slip Distribution along the Lengloling Fault in the NE Tibetan Plateau: Implications for Faulting Behavior. *Journal of Asian Earth Sciences*, 172: 190—207. <https://doi.org/10.1016/j.jseaes.2018.09.008>
- Gupta, A., Scholz, C. H., 2000. A Model of Normal Fault Interaction Based on Observations and Theory. *Journal of Structural Geology*, 22(7): 865—879. [https://doi.org/10.1016/S0191-8141\(00\)00011-0](https://doi.org/10.1016/S0191-8141(00)00011-0)
- Hetzell, R., Hampel, A., Gebbeken, P., et al., 2019. A Constant Slip Rate for the Western Qilian Shan Frontal Thrust during the Last 200 ka Consistent with GPS-Derived and Geological Shortening Rates. *Earth and Planetary Science Letters*, 509: 100—113. <https://doi.org/10.1016/j.epsl.2018.12.032>
- Hu, X. F., Chen, D. B., Pan, B. T., et al., 2019. Sedimentary Evolution of the Foreland Basin in the NE Tibetan Plateau and the Growth of the Qilian Shan since 7 Ma. *GSA Bulletin*, 131(9—10): 1744—1760. <https://doi.org/10.1130/b35106.1>
- Huang, X. N., Yang, X. P., Yang, H. B., et al., 2021. Re-Evaluating the Surface Rupture and Slip Distribution of the AD 1609 $M7 \frac{1}{4}$ Hongyapu Earthquake along the Northern Margin of the Qilian Shan, NW China: Implications for Thrust Fault Rupture Segmentation. *Frontiers in Earth Science*, 9: 633820. <https://doi.org/10.3389/feart.2021.633820>
- Institute of Geology, Lanzhou Institute of Seismology, China Earthquake Administration, 1993. Active Fault Zones in Qilian Mountains and Hexi Corridor Regions. Seismological Press, Beijing (in Chinese).
- Jin, Q., He, W. G., Shi, Z. G., et al., 2011. Palaeo-Earthquake Study on the Northern Yumushan Active Fault. *Seismology and Geology*, 33(2): 347—355 (in Chinese with English abstract).
- Kang, W. J., Xu, X. W., Oskin, M. E., et al., 2020. Characteristic Slip Distribution and Earthquake Recurrence along the Eastern Altyn Tagh Fault Revealed by High-Resolution Topographic Data. *Geosphere*, 16(1): 392—406. <https://doi.org/10.1130/ges02116.1>
- Kang, W. J., Xu, X. W., Yu, G. H., et al., 2020. Comparison Study of Two Kinds of Codes to Measure Fault-Offsets Based on Matlab: A Case Study on Eastern Altyn Tagh Fault. *Seismology and Geology*, 42(3): 732—747 (in Chinese with English abstract).
- Kim, Y. S., Andrews, J. R., Sanderson, D. J., 2000. Damage Zones around Strike-Slip Fault Systems and Strike-Slip Fault Evolution, Crackington Haven, Southwest England. *Geosciences Journal*, 4(2): 53—72. <https://doi.org/10.1007/BF02910127>
- Klinger, Y., Etchebe, M., Tapponnier, P., et al., 2011. Characteristic Slip for Five Great Earthquakes along the Fuyun Fault in China. *Nature Geoscience*, 4(6): 389—392. <https://doi.org/10.1038/ngeo1158>
- Liang, S. M., Gan, W. J., Shen, C. Z., et al., 2013. Three-

- Dimensional Velocity Field of Present-Day Crustal Motion of the Tibetan Plateau Derived from GPS Measurements. *Journal of Geophysical Research: Solid Earth*, 118(10): 5722–5732. <https://doi.org/10.1002/2013jb010503>
- Liu, J., Chen, T., Zhang, P. Z., et al., 2013. Illuminating the Active Haiyuan Fault, China by Airborne Light Detection and Ranging. *Chinese Science Bulletin*, 58(1): 41–45 (in Chinese).
- Liu, X. W., Yuan, D. Y., Zheng, W. J., et al., 2019. Holocene Slip Rate of the Frontal Thrust in the Western Qilian Shan, NE Tibetan Plateau. *Geophysical Journal International*, 219(2): 853–865. <https://doi.org/10.1093/gji/ggz325>
- Manighetti, I., Campillo, M., Bouley, S., et al., 2007. Earthquake Scaling, Fault Segmentation, and Structural Maturity. *Earth and Planetary Science Letters*, 253(3–4): 429–438. <https://doi.org/10.1016/j.epsl.2006.11.004>
- Manighetti, I., Campillo, M., Sammis, C., et al., 2005. Evidence for Self-Similar, Triangular Slip Distributions on Earthquakes: Implications for Earthquake and Fault Mechanics. *Journal of Geophysical Research: Solid Earth*, 110(B5): B05302. <https://doi.org/10.1029/2004jb003174>
- Manighetti, I., Caulet, C., de Barros, L., et al., 2015. Generic Along-Strike Segmentation of Afar Normal Faults, East Africa: Implications on Fault Growth and Stress Heterogeneity on Seismogenic Fault Planes. *Geochemistry, Geophysics, Geosystems*, 16(2): 443–467. <https://doi.org/10.1002/2014gc005691>
- Manighetti, I., Perrin, C., Gaudemer, Y., et al., 2020. Repeated Giant Earthquakes on the Wairarapa Fault, New Zealand, Revealed by Lidar-Based Paleoseismology. *Scientific Reports*, 10(1): 2124. <https://doi.org/10.1038/s41598-020-59229-3>
- Palumbo, L., Hetzel, R., Tao, M. X., et al., 2009. Deciphering the Rate of Mountain Growth during Topographic Presteady State: An Example from the NE Margin of the Tibetan Plateau. *Tectonics*, 28(4): C4017. <https://doi.org/10.1029/2009tc002455>
- Pang, W., He, W. G., Zhang, B., 2019. Preliminary Study of New Faulting Characteristic of the Linze Fault. *Journal of Seismological Research*, 42(1): 120–132 (in Chinese with English abstract).
- Philip, H., Rogozhin, E., Cisternas, A., et al., 1992. The Armenian Earthquake of 1988 December 7: Faulting and Folding, Neotectonics and Palaeoseismicity. *Geophysical Journal International*, 110(1): 141–158. <https://doi.org/10.1111/j.1365-246X.1992.tb00718.x>
- Ren, J. J., Xu, X. W., Zhang, S. M., et al., 2019. Late Quaternary Slip Rates and Holocene Paleoearthquakes of the Eastern Yumu Shan Fault, Northeast Tibet: Implications for Kinematic Mechanism and Seismic Hazard. *Journal of Asian Earth Sciences*, 176: 42–56. <https://doi.org/10.1016/j.jseas.2019.02.006>
- Ren, Z. K., Zhang, Z. Q., Chen, T., et al., 2016. Clustering of Offsets on the Haiyuan Fault and Their Relationship to Paleoearthquakes. *Geological Society of America Bulletin*, 128(1–2): 3–18. <https://doi.org/10.1130/b31155.1>
- Scholz, C. H., Dawers, N. H., Yu, J. Z., et al., 1993. Fault Growth and Fault Scaling Laws: Preliminary Results. *Journal of Geophysical Research: Solid Earth*, 98(B12): 21951–21961. <https://doi.org/10.1029/93jb01008>
- Segall, P., Pollard, D. D., 1980. Mechanics of Discontinuous Faults. *Journal of Geophysical Research: Solid Earth*, 85: 4337–4350. <https://doi.org/10.1029/JB085iB08p04337>
- Stewart, N., Gaudemer, Y., Manighetti, I., et al., 2018. “3D_Fault_Offsets,” a Matlab Code to Automatically Measure Lateral and Vertical Fault Offsets in Topographic Data: Application to San Andreas, Owens Valley, and Hope Faults. *Journal of Geophysical Research: Solid Earth*, 123(1): 815–835. <https://doi.org/10.1002/2017jb014863>
- Ta, W. Q., Xiao, H. L., Qu, J. J., et al., 2004. Measurements of Dust Deposition in Gansu Province, China, 1986–2000. *Geomorphology*, 57(1–2): 41–51. [https://doi.org/10.1016/S0169-555X\(03\)00082-5](https://doi.org/10.1016/S0169-555X(03)00082-5)
- Tapponnier, P., Meyer, B., Avouac, J. P., et al., 1990. Active Thrusting and Folding in the Qilian Shan, and Decoupling between Upper Crust and Mantle in Northeastern Tibet. *Earth and Planetary Science Letters*, 97(3–4): 382–383, 387–403. [https://doi.org/10.1016/0012-821X\(90\)90053-Z](https://doi.org/10.1016/0012-821X(90)90053-Z)
- Wei, Z. Y., He, H. L., Sun, W., et al., 2020. Investigating Thrust-Fault Growth and Segment Linkage Using Displacement Distribution Analysis in the Active Duzhanzi Thrust Fault Zone, Northern Tian Shan of China. *Journal of Structural Geology*, 133: 103990. <https://doi.org/10.1016/j.jsg.2020.103990>
- Wesnousky, S. G., 2008. Displacement and Geometrical Characteristics of Earthquake Surface Ruptures: Issues and Implications for Seismic-Hazard Analysis and the Process of Earthquake Rupture. *Bulletin of the Seismological Society of America*, 98(4): 1609–1632. <https://doi.org/10.1785/0120070111>
- Wilkins, S. J., Gross, M. R., 2002. Normal Fault Growth in

- Layered Rocks at Split Mountain, Utah: Influence of Mechanical Stratigraphy on Dip Linkage, Fault Restriction and Fault Scaling. *Journal of Structural Geology*, 24(9): 1413—1429. [https://doi.org/10.1016/S0191-8141\(01\)00154-7](https://doi.org/10.1016/S0191-8141(01)00154-7)
- Xiong, J. G., Li, Y. L., Zhong, Y. Z., et al., 2017. Latest Pleistocene to Holocene Thrusting Recorded by a Flight of Strath Terraces in the Eastern Qilian Shan, NE Tibetan Plateau. *Tectonics*, 36(12): 2973—2986. <https://doi.org/10.1002/2017tc004648>
- Xu, X. W., Wen, X. Z., Yu, G. H., et al., 2009. Coseismic Reverse- and Oblique-Slip Surface Faulting Generated by the 2008 Mw 7.9 Wenchuan Earthquake, China. *Geology*, 37(6): 515—518. <https://doi.org/10.1130/G25462A.1>
- Xu, X. W., Yeats, R. S., Yu, G. H., 2010. Five Short Historical Earthquake Surface Ruptures near the Silk Road, Gansu Province, China. *Bulletin of the Seismological Society of America*, 100(2): 541—561. <https://doi.org/10.1785/0120080282>
- Yang, H. B., Yang, X. P., Huang, X. N., et al., 2018. New Constraints on Slip Rates of the Fodongmiao-Hongyazi Fault in the Northern Qilian Shan, NE Tibet, from the ¹⁰Be Exposure Dating of Offset Terraces. *Journal of Asian Earth Sciences*, 151: 131—147. <https://doi.org/10.1016/j.jseaes.2017.10.034>
- Yang, S. F., Chen, H. L., Cheng, X. G., et al., 2007. Deformation Characteristics and Rules of Spatial Change for the Northern Qilianshan Thrust Belt. *Earth Science Frontiers*, 14(5): 211—221 (in Chinese with English abstract).
- Yao, W. Q., Jing, L. Z., Osokin, M. E., et al., 2019. Re-evaluation of the Late Pleistocene Slip Rate of the Haiyuan Fault near Songshan, Gansu Province, China. *Journal of Geophysical Research: Solid Earth*, 124(5): 5217—5240. <https://doi.org/10.1029/2018jb016907>
- Ye, Z., Gao, R., Li, Q. S., et al., 2015. Seismic Evidence for the North China Plate Underthrusting beneath Northeastern Tibet and Its Implications for Plateau Growth. *Earth and Planetary Science Letters*, 426: 109—117. <https://doi.org/10.1016/j.epsl.2015.06.024>
- Yu, G. H., Xu, X. W., Klinger, Y., et al., 2010. Fault-Scarp Features and Cascading-Rupture Model for the Mw 7.9 Wenchuan Earthquake, Eastern Tibetan Plateau, China. *Bulletin of the Seismological Society of America*, 100(5B): 2590—2614. <https://doi.org/10.1785/0120090255>
- Zhang, P. Z., Mao, F. Y., Slemmons, D. B., 1999. Rupture Terminations and Size of Segment Boundaries from Historical Earthquake Ruptures in the Basin and Range Province. *Tectonophysics*, 308(1—2): 37—52. [https://doi.org/10.1016/S0040-1951\(99\)00089-X](https://doi.org/10.1016/S0040-1951(99)00089-X)
- Zhang, P. Z., Shen, Z. K., Wang, M., et al., 2004. Continuous Deformation of the Tibetan Plateau from Global Positioning System Data. *Geology*, 32(9): 809—812. <https://doi.org/10.1130/g20554.1>
- Zheng, W. J., Zhang, P. Z., He, W. G., et al., 2013. Transformation of Displacement between Strike-Slip and Crustal Shortening in the Northern Margin of the Tibetan Plateau: Evidence from Decadal GPS Measurements and Late Quaternary Slip Rates on Faults. *Tectonophysics*, 584: 267—280. <https://doi.org/10.1016/j.tecto.2012.01.006>
- Zielke, O., Arrowsmith, J. R., Ludwig, L. G., et al., 2010. Slip in the 1857 and Earlier Large Earthquakes along the Carrizo Plain, San Andreas Fault. *Science*, 327(5969): 1119—1122. <https://doi.org/10.1126/science.1182781>
- Zuza, A. V., Cheng, X. G., Yin, A., 2016. Testing Models of Tibetan Plateau Formation with Cenozoic Shortening Estimates across the Qilian Shan-Nan Shan Thrust Belt. *Geosphere*, 12(2): 501—532. <https://doi.org/10.1130/ges01254.1>

附中文参考文献

- 陈宣华, 邵兆刚, 熊小松, 等, 2019. 祁连山北缘早白垩世榆木山逆冲推覆构造与油气远景. 地球学报, 40(3): 377—392.
- 中国地震局地质研究所, 中国地震局兰州地震研究所. 1993. 祁连山-河西走廊活动断裂系. 北京: 地震出版社.
- 金卿, 何文贵, 史志刚, 等, 2011. 榆木山北缘断裂古地震特征研究. 地震地质, 33(2): 347—355.
- 康文君, 徐锡伟, 于贵华, 等, 2020. 2种基于Matlab平台的断层位移测量软件对比分析: 以阿尔金断裂东段为例. 地震地质, 42(3): 732—747.
- 刘静, 陈涛, 张培震, 等, 2013. 机载激光雷达扫描揭示海原断裂带微地貌的精细结构. 科学通报, 58(1): 41—45.
- 庞炜, 何文贵, 张波, 2019. 临泽断裂新活动特征初步研究. 地震研究, 42(1): 120—132.
- 杨树锋, 陈汉林, 程晓敢, 等, 2007. 祁连山北缘冲断带的特征与空间变化规律. 地学前缘, 14(5): 211—221.